

# Using Graph Theory to Represent Brittle Plane Networks

Soumyajit Mukherjee

Department of Earth Sciences, Indian Institute of Technology Bombay, Powai, Mumbai, India

## OUTLINE

1 Background	259	Acknowledgments	270
2 Graph Theory	260	Appendix	271
Solutions	268	References	271

*“Outcrop studies are used to characterise fracture patterns within potential hydrocarbon reservoir units, with the expectation that these data will positively enhance the development of fractured reservoirs...” – Watkins et al. (2015).*

## 1 BACKGROUND

Graph theory deals with connection amongst points (vertices/nodes) by edges/lines. The theory finds great use in computer science. This chapter exemplifies the concept of graph theory in the context of brittle plane (fractures and faults) networks. It is important to demonstrate use of language of one scientific discipline into another. The comparison and use is restricted to geometry only and does not involve genesis. Not each and every term of graph theory is explained/used here. The idea is to give students an introduction through examples. Problems posed for students are in bold and are inside the main text itself. This chapter can work as a primer for those who want to model fluid flow through fracture networks.

Several approaches and terms exist to describe network of planes in geosciences.

Brittle plane topology can depend on several factors: strain variation, temporal reorientation/deflection of stress, and fabric inheritance (Morley and Nixon, 2016). Representation of homogeneous fractures is easy but is not so when the fractures are heterogeneous (Watkins et al., 2015).

Planes in space can be divided into three types based on their connectivity: I, Y, and X pattern. With reference to the definition of types of nodes in Fig. 1, the percentages of I-, Y-, and X-nodes of faults can vary from terrain to terrain (Morley and Nixon, 2016). The relative populations/samples of these three kinds of nodes of fractures can be presented in triangular graphs (e.g., Fig. 7 of Laubach et al., 2018). Splay faulting is like the “Y-node pattern” (Peacock et al., 2016). Y-nodes were sub-divided further by Morley and Nixon (2016) into splaying ( $Y_s$ ), abutting ( $Y_a$ ), and cross-cutting ( $Y_c$ ) types. The node frequency ( $N_N$ ) is given by (Procter and Sanderson, 2018):

$$N_N = (N_I + N_Y + N_X) \quad (1)$$

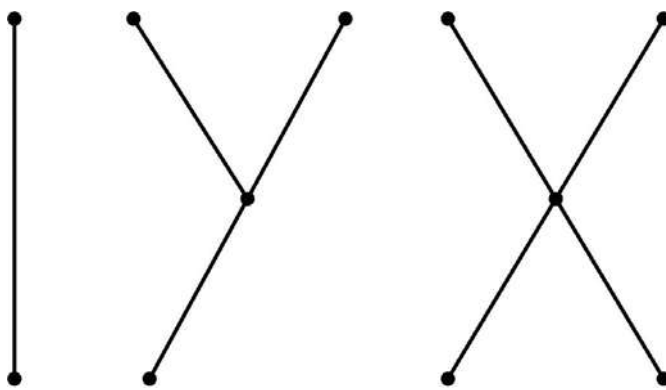


FIG. 1 Definition of I, Y, and X nodes.

The number of branches ( $N_B$ ) is given by (Procter and Sanderson, 2018):

$$N_B = 0.5 \times (N_I + 3N_Y + 4N_X) \quad (2)$$

Synkinematic cementation can cluster fractures. Fracture clustering can also be due to (i) folding, (ii) faulting, (iii) dyke propagation, and (iv) diagenesis (review in Hooker et al., 2018). Macrofractures are commonly associated with microfractures. Fracture network understanding is essential in studying fractured reservoirs (Watkins et al., 2018). Isolated fracture networks, which are poor conductors of fluids, exist in rocks (Fig. 1C of Watkins et al., 2015). The unit-less ratio of number of connected to the number of unconnected nodes is called the “connectivity” (Petford and Koenders, 1998). Petford and Koenders (1998) described temporal increase in connectivity amongst fractures in natural situations. Besides conventional studies in the field and those using optical microscope, UAV and SfM photogrammetry techniques have been recently used to study large-scale (>20 m) fractures (Bemis et al., 2014; Corradetti et al., 2018).

The purpose of this chapter is to introduce the graph theory concept to geoscience students so that they themselves can proceed in detail aspects if they want so. Origin of graph theory and its diverse use in geosciences has been reviewed briefly in Howarth (2017). These include cartography, fracture analyses, flow through fractured media, etc. This article can have a far-reaching implication in reservoir geomechanics such as Li (2017) in terms of quantifying fracture and fault orientation in space (e.g., Marrett et al., 2018). Interestingly, Sanderson et al. (in press) recently presented definitions of elements in graph theory using geological examples.

## 2 GRAPH THEORY

The *graph theory* studies connection amongst several points, either in 2D or in 3D, and usually represents them in terms of a binary code inside matrices (Pal and Das, 2017). Such connections may not always have a physical link, for example, connection between two mobile phones or the atomic bonds in chemistry.

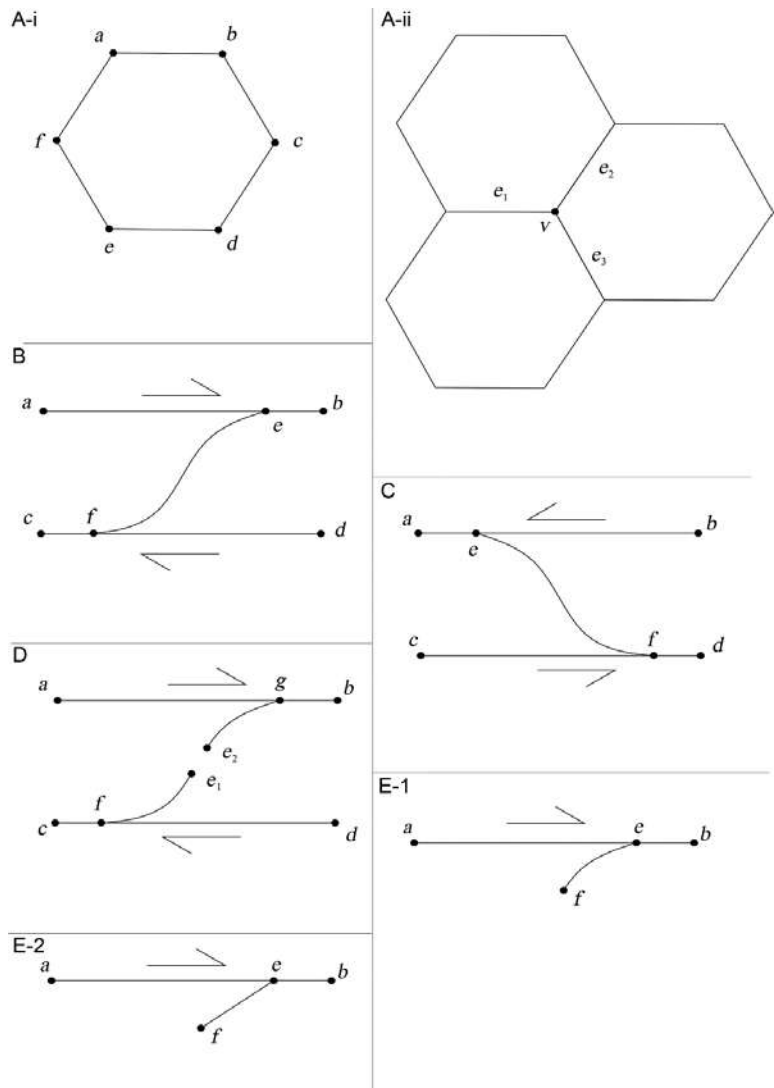
In structural geology and geomechanics, diverse fracture and fault geometries and their connectivity have been already described (many presented in Mukherjee, 2013a, 2014a,b, 2015). This study uses graph theory to represent a number of well-known fracture patterns. The idea is to show how far terminologies of graph theory can be used in structural geological contexts. Besides those used in this chapter, many other terminologies exist in graph theory texts (e.g., Bollobas, 1998; Goehring et al., 2014), and those can be also attempted to fit into structural geology.

Connected points along with their connections constitute *graphs*. Either straight or curved lines can represent these connections. The points are called *nodes* or *vertices*, and the connecting lines are *edges*. The edges can be straight or curved lines. The set of vertices or nodes ( $V$  or  $N$ ) are called a *vertex or node set*. Similarly *edge sets* ( $E$ ) are defined. A graph is represented by  $G(V,E)$ . The length and curvature of edges are commonly not reflected in  $G$ .

Take examples of polygonal fracture patterns as found in desiccation cracks and in columnar joints in cross-sections (Fig. 2A-i). Here, vertex set  $V: \{a,b,c,d,e,f\}$  and edge set  $E: \{ab, bc, cd, de, ef\}$ . The graph is therefore  $G: [\{a,b,c,d,e,f\}, \{ab, bc, cd, de, ef, fa\}]$ . A desiccation crack or a columnar fracture can have a number of sides/edges different than 6, but in all such cases,  $V$ ,  $E$  and  $G$  can be defined.

Similarly, for a brittle shear zone with  $Y$  and  $P$  planes indicating a top-to-right shear (Fig. 2B)  $G: [\{a,b,c,d,e,f\}, \{ae, eb, ef, cf, fd\}]$ . Note that  $G$  remains the same for a top-to-left brittle shear as well (Fig. 2C). For a brittle shear zone, where one of

FIG. 2 (A-i and A-ii) Polygonal fracturing; (B) Top-to-right brittle shear zone; (C) Top-to-left brittle shear zone; (D, E-i, E-ii): Immature brittle shear zone.



the nodes of the  $P$ -planes do not touch the  $Y$ -plane (Fig. 2D),  $G$ : would be represented by  $[\{a, g, b, c, f, d, e_1, e_2\}, \{ae, eb, ef, cf, fd, ge_2, fe_1\}]$ . With pronounced brittle shear,  $ge_2$  and  $fe_1$  can migrate toward  $e_2$  and  $e_1$  directions, respectively, so that  $ge_2$  and  $fe_1$  may join to form a single curved  $P$ -brittle plane, which will look same as Fig. 2B. In that case,  $e_1$  and  $e_2$  nodes will not possess any significance, and the resultant graph  $G$  will be same as that for Fig. 2B. Note Fig. 2D case has two nodes and one edge more than the Fig. 2B case. Thus graphs for specific structures can modify temporally as the structures evolve, and new connections develop between points.

Even if the  $Y$ -planes are a bit curved, or say the  $P$ -plane is rather straight, the graphs do not alter. For example, the graph  $G$  for Fig. 2E-1 and E-2 are the same. Single brittle shear zones do show variation in curvature in  $Y$ - and  $P$ -planes spatially (e.g., Mukherjee, 2013b). Note pronounced brittle shear can make  $P$  and  $Y$  planes nearly sub-parallel, and in that case, defining nodes such as  $e$  and  $f$  in Fig. 2B can become difficult.

The two end points of an edge are called *end vertices*. Therefore for example, in Fig. 2B, the end vertices for edges  $ab$  and  $cd$  are  $\{a, b\}$  and  $\{c, d\}$ , respectively.

Depending on different sets or generations of brittle planes, one can divide/categorize vertices and edges. In Fig. 2B's case of brittle shear,  $V: \{V_p, V_Y\}$  and  $E: \{E_p, E_Y\}$ , where  $V_p: \{e, f\}$ ,  $V_Y: \{a, b, e, c, f, d\}$ ,  $E_p: \{ef\}$ ,  $E_Y: \{ae, eb, cf, fd\}$ . Here  $P$  and  $Y$  subscripts indicate vertices and edges related to  $P$ - and  $Y$ -planes, respectively.  $V$  and  $E$  are called *supersets* and  $V_p, V_Y, E_p$  and  $E_Y$  *subsets*. But what has been proven to be a simple classification of subsets in brittle shear zones will not always be possible if geological information about fractures of different attitudes are not known, or if theoretically it is established that fractures with different trends develop near-coevally. For example, in the case of desiccation cracks

(Fig. 2A-i), subsets cannot be established. This is because we commonly believe that the edges  $ab$ ,  $bc$ ,  $cd$ ,  $de$ ,  $ef$ , and  $fa$  developed simultaneously.

Two edges with common vertices are called *parallel edges*. Such edges may or may not be straight and parallel lines. Fig. 3 is a top-to-left shear induced pull-apart basin. Edges  $e_1$  and  $e_2$  are parallel because they have common vertices  $V_1$  and  $V_2$ .

Spheroidal weathering-related atectonic fractures are sub-circular or sub-elliptical (Fig. 4A), with a single edge and a conceptual vertex. Such a graph can be called a *loop* or a *self loop*. A graph constituting a loop is not called a simple graph. Graphs with no loops and no parallels (Fig. 2A-E) are called *simple graphs*. Therefore the polygonal fractures and brittle shear examples constitute simple graphs.

Few terms exist that correlates edges with vertices. For example, *adjacent edges* are nonparallel edges with common vertex. The  $P$ - and the  $Y$ -planes always constitute adjacent edges, because in Fig. 2B, the  $Y$ -plane edges  $ae$  and the  $P$ -plane edge  $ef$  have a common vertex  $e$ . This is also true for the formative stages of  $P$ -planes (Fig. 2D) when one of the vertices of the  $P$ -plane edges  $e_2g$  and  $e_1g$  do not touch the  $Y$ -plane.

The number of edges incident to a vertex with the loop taken twice is called the *degree of the vertex*. Therefore degree of the vertex defined by the intersection between the  $P$ - and the  $Y$ -planes, such as vertices  $e$  and  $f$  in Fig. 2B, have degree = 3. This is because three edges  $ae$ ,  $eb$  (defining the  $Y$ -plane), and  $ef$  (defining the  $P$ -plane) have the common vertex  $e$ . A similar argument works for vertex  $f$  and the edges  $af$ ,  $df$ , and  $ef$ . Immature brittle shear zones with one of the nodes of the  $P$ -planes unconnected with the  $Y$ -plane (Fig. 2D), such as nodes  $e_1$  and  $e_2$  for the edges  $e_1f$  and  $e_2g$  edges have degree = 1. We can say therefore that with progressive deformation, the degree of vertices can modify as those vertices get new connections. Vertices  $e$  in Fig. 2B and  $e_i$  ( $i=1, 2$ ) in Fig. 2D can be called *odd vertices* as their degrees are odd numbers. If not, they would have been called *even vertices*. Thus for both mature and immature ideal brittle shear zones, all the vertices are odd.

If a single graph has different degrees for its different vertices, that graph is called *irregular*. Therefore both the immature and mature brittle shear zones constitute irregular graphs. A graph with the same degree for all its vertices is a *regular graph*. Polygonal fractures (Fig. 2A-i) is a regular graph with every vertices with degree 2. This is because, for example, edges  $ab$  and  $bc$  are incident on the common vertex  $b$ . A set of sub-parallel fractures (Fig. 4B) can be called *pendant edges* individually because their vertices have degree = 1. Such vertices are also called *pendant vertices*.

An *isolated vertex* is not connected to any edges and would be simply a point representation. A very tiny fracture with no visible length in mesoscale can be called an isolated vertex, with degree = 0, and such a graph would be called a *null graph*. However, in microscale, a length of such a fracture can be deciphered. Therefore use of the term "isolated vertex" in structural geology would be scale-dependent.

If two adjacent edges have a common vertex with degree = 2, those edges are said to be in a *series*. For a mature shear zone (Fig. 2B), no two edges are in series because none of their vertices have degree = 2. To be precise,  $deg(e) = deg(f) = 3$ , and  $deg(a) = deg(b) = deg(c) = deg(d) = 1$ . The immature shear zones (Fig. 2D) also do not have edges in series, because  $deg(a) = deg(b) = deg(c) = deg(d) = deg(e_1) = deg(e_2) = 1$ , and  $deg(f) = deg(g) = 3$ .

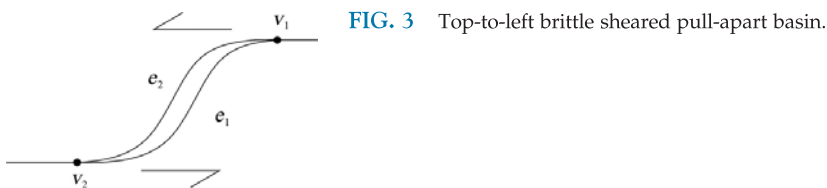


FIG. 3 Top-to-left brittle sheared pull-apart basin.

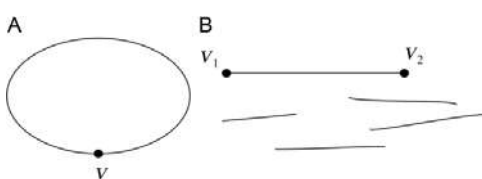


FIG. 4 (A) Spheroidal weathering generated fracture. (B) Sub-parallel fracture or fault set.

Now consider the polygonal fracturing case (Fig. 2A-i). Here, considering a hexagon, all the edges  $ab, bc, cd, \dots, fa$  are incident on vertices  $b, c, \dots, a$  with degree 2. Therefore all of its edges are in series. The same holds true for polygons of any number of sides  $>$  or  $<6$ . However, if one considers a number of polygonal fractures connected (Fig. 2A-ii), some of the vertices, for example,  $v$  has degree = 3 because adjacent edges  $e_i$  ( $i = 1, 2, 3$ ) are connected with this. Therefore edges  $e_i$  themselves are not in series.

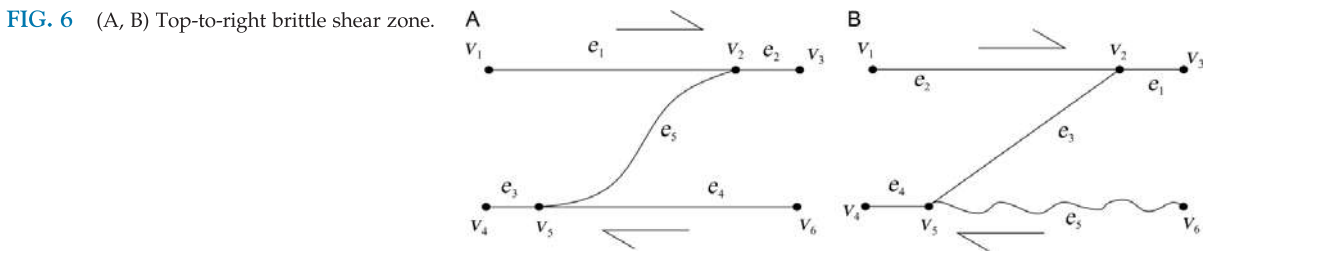
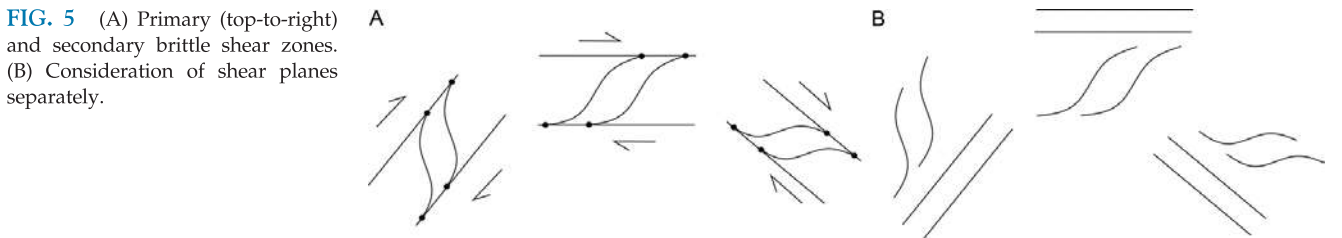
A *complete graph* is one where all the vertices are connected by edges. The polygonal fractures (Fig. 2A-i) do not constitute a complete graph because edges  $ae, ad$ , etc. do not exist. The mature (Fig. 2B) and immature shear zones (Fig. 2D) are also not complete graphs because, in both the cases, vertices such as  $a$  and  $c$ , and  $b$  and  $d$  are not connected by any edges. Only in the spheroidal weathering case (Fig. 4), all the vertices (one here) are connected by edge  $e$ . Therefore it is a complete graph.

$G_1(V_1, E_1)$  is a *sub-graph* of the *supergraph*  $G(V, E)$  if  $V_1$  and  $E$  are sub-sets of  $V$  and  $U$ , respectively. Taking Fig. 2B as a supergraph, one can think of the vertices and edges required to draw the  $P$ -plane, that is, vertices  $e$  and  $f$ , and the edge  $ef$  as a sub-graph. On the other hand, if one takes vertices  $a, e, f$ , and  $c$  and the edges  $ae, ef$ , and  $fc$ , it will not make any meaningful sub-group geologically, because it could not separate two sets of planes  $P$  and  $Y$ , but instead it considered both. On the other hand, defining any single sub-group from polygonal fractures (Fig. 2A-i) would not be meaningful. One can consider a brittle shear zone with primary ( $Y$  and  $P$ ) and secondary shear planes ( $P, R$ , and  $R'$ ) as a supergraph. Individually, those primary and secondary shear planes constitute separate sub-graphs (Fig. 5A). We can also define geologically meaningful sub-sub-graphs (Fig. 5B).

The sub-graph  $G_1$  of  $G$  is called a *spanning sub-graph* if  $G_1$  and  $G$  have same vertices. *Can you think of a meaningful geological example of a spanning sub-graph?* Two graphs can be called *vertex disjoint* if they have no common vertices. With reference to Fig. 2E-2, one can think of only the  $P$ -plane consisting of the edge  $ef$  and the vertices  $e$  and  $f$  as a separate graph  $G_P$ , and the  $Y$ -plane consisting of the edges  $ae$  and  $eb$  along with the vertices  $a, e$ , and  $b$  as a separate graph  $G_Y$ . However,  $G_P$  and  $G_Y$  are *not* vertex disjoint because they have a common vertex  $e$ . Two graphs are called *edge disjoint* if they do not have common edge(s).  $G_P$  and  $G_Y$  are edge disjoint graphs.

The *union* and *intersection* of graphs can now be explained (Fig. 2B). Say there are two graphs  $G_Y$  with vertex set  $\{a, e, b, c, f, d\}$  and edge set  $\{ab, cd\}$  and  $G_P$  with  $\{e, f\}$  and  $\{ef\}$ , respectively. Now  $G_Y \cup G_P$  would represent Fig. 2B itself.  $G_Y \cap G_P$  is merely the vertex set  $\{e, f\}$ .

If a graph is defined by edges joining several nodes, the *complement* of that graph is defined by the same vertex set but differently joined edges. In the context of brittle shear zones, complement of a graph defined by  $G_P$  and  $G_Y$  if visualized by joining lines in Fig. 6A have *no* physical meaning. If at least two vertices exist in a graph, which are not connected by a path, we call such a graph *disconnected*. The geological cases for Fig. 2A-i and B, etc. are, conversely, *connected graphs* because paths exist for any two vertices. However, for an immature shear zone (Fig. 2D), vertices  $e_1$  and  $e_2$  have no paths. Therefore Fig. 1D represents a disconnected graph. As can be seen, such a graph can be



considered to be constituted of two sub-graphs, and in this case, the supergraph is said to have two *components*. A *walk* or a *chain* is the sequence of vertices and edges one needs to cross to reach one vertex to the other. In Fig. 2B, *a-b* walk is:  $a, ae, e, eb$ . In the same figure, *c-b* walk is  $c, cf, f, fe, e, fb, b$ . The number of edges encountered in a walk is called the *length of walk*. Therefore for *a-b* walk, the length is 2, and that for the *c-b* walk, it is 3. The two referred walks are called *open walk* because their starting and the ending vertices differ. If this is not the case, such as the polygonal fracture case in Fig. 2A-i, then the *a-a* walk:  $a, ab, b, bc, c, cd, d, de, e, ef, f, fa, a$  is a *close walk*. The previously mentioned cases of open and close walks can also be called *trials* or *circuits* because no edges came twice. Likewise, the *a-b* walk can be called a *path* or a *simple path* because no vertices occur more than once.

The *distance between vertices* is the length of the shortest path between two vertices when tracked on the straight or curved edges. Thus the distance between points  $a$  and  $c$  (Fig. 2A-i) is the sum of the distances  $ab$  and  $bc$ , and is neither  $ac$  nor  $af+fe+ed+dc$ . Note the edge can be imaginary, that is, no fracture joins edges  $e$  and  $f$ . In case of brittle shear zone (Fig. 2B), this distance between vertices  $e$  and  $f$ , is the curved length of the  $P$ -plane, which has a physical meaning. The maximum distance measured along edges between any two points is called the *diameter of the graph*. Therefore for a symmetric hexagonal fracturing with all sides equal (Fig. 2A), the same diameter exists for several two vertices such as between  $a$  and  $b$  given by  $af+fe+ed+dc+cb$ , which is same as those for vertices  $d$  and  $e$  given by  $ef+fa+ab+bc+cd$ .

The number of vertices ( $v$ ), edges ( $e$ ), and components ( $k$ ) of a graph are called its *fundamental numbers*. Magnitudes of  $v$ ,  $e$  and  $k$  are independent. In Fig. 2D,  $n=6$ ,  $e=5$ , and  $k=2$ . *Rank of a graph*  $R = (n - k)$ . In this case  $R = 4$ . The nullity of the graph is defined as  $N = (e - R)$ . In this case  $N = 1$ . Note that the fundamental numbers ( $v$ ,  $e$ , and  $k$ ) do not represent the geometry uniquely.

Graphs, and therefore brittle plane networks, can be represented by matrices. One can construct an *incidence matrix* with vertices written as columns and edges as rows as shown here. If a vertex is incident on the edge, the corresponding matrix element is "1". If not, "0" is the element. With a different notation of Fig. 2B as Fig. 6A, its binary matrix representation would be,  $A_1(G)$ :

	$e_1$	$e_2$	$e_3$	$e_4$	$e_5$
$v_1$	1	0	0	0	0
$v_2$	1	1	0	0	1
$v_3$	0	1	0	0	0
$v_4$	0	0	1	0	0
$v_5$	0	0	1	1	0
$v_6$	0	0	0	1	0

Note the number of rows may or may not equal that of columns in such matrices.

**Q. 1A. Construct an incidence matrix for Fig. 2D.**

**Q. 1B. Draw a situation where one of the rows of an incident matrix is represented by only "0".**

**Q. 1C. Draw a geological case of brittle plane network where one of the rows is represented by only '1'. In other words, draw a geological case where all the edges are linked with a single vertex.**

The incidence matrix  $A(G)$  of two disconnected graphs  $G_1$  and  $G_2$  is given by:

$$A(G) = \begin{pmatrix} A(G_1) & 0 \\ 0 & A(G_2) \end{pmatrix}$$

Here 0 is the null matrix.  $A(G_2)$  is given by:

	$e_1$	$e_2$	$e_3$	$e_4$	$e_5$
$v_1$	1	0	0	0	0
$v_2$	1	1	0	0	1
$v_3$	0	1	0	0	0
$v_4$	0	0	1	0	1
$v_5$	0	0	1	1	0
$v_6$	0	0	0	1	0

Say  $A(G_3)$  is given by:

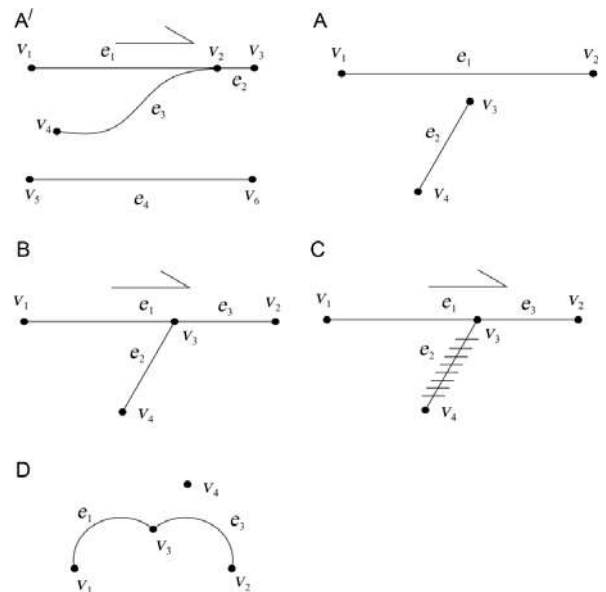
	$e_6$	$e_7$	$e_8$	$e_9$	$e_{10}$
$v_7$	1	0	0	0	0
$v_8$	1	1	0	0	1
$v_9$	0	1	0	0	0
$v_{10}$	0	0	1	0	0
$v_{11}$	0	0	1	1	1
$v_{12}$	0	0	0	1	0

Therefore  $A(G)$ :

	$e_1$	$e_2$	$e_3$	$e_4$	$e_5$	$e_6$	$e_7$	$e_8$	$e_9$	$e_{10}$
$v_1$	1	0	0	0	0	<b>0</b>	<b>0</b>	<b>0</b>	<b>0</b>	<b>0</b>
$v_2$	1	1	0	0	1	<b>0</b>	<b>0</b>	<b>0</b>	<b>0</b>	<b>0</b>
$v_3$	0	1	0	0	0	<b>0</b>	<b>0</b>	<b>0</b>	<b>0</b>	<b>0</b>
$v_4$	0	0	1	0	1	<b>0</b>	<b>0</b>	<b>0</b>	<b>0</b>	<b>0</b>
$v_5$	0	0	1	1	0	<b>0</b>	<b>0</b>	<b>0</b>	<b>0</b>	<b>0</b>
$v_6$	0	0	0	1	0	<b>0</b>	<b>0</b>	<b>0</b>	<b>0</b>	<b>0</b>
$v_7$	<b>0</b>	<b>0</b>	<b>0</b>	<b>0</b>	<b>0</b>	1	0	0	0	0
$v_8$	<b>0</b>	<b>0</b>	<b>0</b>	<b>0</b>	<b>0</b>	1	1	0	0	1
$v_9$	<b>0</b>	<b>0</b>	<b>0</b>	<b>0</b>	<b>0</b>	0	1	0	0	0
$v_{10}$	<b>0</b>	<b>0</b>	<b>0</b>	<b>0</b>	<b>0</b>	0	0	1	0	0
$v_{11}$	<b>0</b>	<b>0</b>	<b>0</b>	<b>0</b>	<b>0</b>	0	0	1	1	1
$v_{12}$	<b>0</b>	<b>0</b>	<b>0</b>	<b>0</b>	<b>0</b>	0	0	0	1	0

“0” in bold represents the null matrices. Sometimes  $V_i$  and  $e_i$  are not written in the incidence matrices, and only 1 and 0 are written.  $A(G)$  can be understood easily. Because  $G_2$  and  $G_3$  are disconnected graphs,  $e_i$  of  $G_2$  is not connected with  $v_i$  of  $G_3$ ; and  $e_i$  of  $G_3$  is not connected with  $v_i$  of  $G_2$ . In different geological cases, the number of rows and columns of  $G_2$  and  $G_3$  can differ. In Fig. 7A', with pre-existing brittle planes, brittle shear took place along only few planes.

FIG. 7 (A–C) Top-to-right brittle shear zone. (C) The edge  $e_2$  is clay-filled. (D) A graph.



**Q.2. Construct the incidence matrix for  $G_2$ ,  $G_3$  and  $G$  in Fig. 7A'.**

During temporal evolution of fracture networks, fractures may propagate and connect mutually, and at their point of connection, a new vertex can be thought to have formed. Also, processes such as secondary mineralization can seal fracture(s) thereby diminishing permeability. Third, new fractures can develop. In these three cases, the incidence matrix of the network would modify.

**Q.3. Construct the incidence matrix of the supergraph in case of Fig. 7B. This is the case when the node  $v_3$  of Fig. 7A migrated and got arrested at  $e_1$ .****Q.4. Construct the incidence matrix of the supergraph in case of Fig. 7C where the fracture represented by the edge  $e_2$  is partly or completely clogged by secondary mineralization and fluid cannot pass from  $v_4$  to  $v_3$  and vice versa.**

The incidence matrix however cannot alone specify the fracture geometry. For example, the incidence matrices for Fig. 7C and D are the same.

Mutually replacing elements of rows (or columns) of the graph of an incidence matrix is called the *permutation of rows* (or, *permutation of columns*) operation in graph theory, and this produces *isomorphic graphs*. Recall the incidence matrix  $A_1(G)$  for Fig. 6A:

	$e_1$	$e_2$	$e_3$	$e_4$	$e_5$
$v_1$	1	0	0	0	0
$v_2$	1	1	0	0	1
$v_3$	0	1	0	0	0
$v_4$	0	0	1	0	1
$v_5$	0	0	1	1	0
$v_6$	0	0	0	1	0

We interchange the elements for columns  $e_2$  and  $e_3$ , as shown here in bold:

	$e_1$	$e_2$	$e_3$	$e_4$	$e_5$
$v_1$	1	0	0	0	0
$v_2$	1	<b>0</b>	<b>1</b>	0	1
$v_3$	0	<b>0</b>	<b>1</b>	0	0
$v_4$	0	<b>1</b>	<b>0</b>	0	1
$v_5$	0	<b>1</b>	<b>0</b>	1	0
$v_6$	0	0	0	1	0

Maintaining the same location of the vertices and rest of the edges, if we draw a graph from this matrix, we can derive an isomorphous graph. Fig. 6A and B are isomorphous graphs. Note that  $e_1$  and the  $e_2$  are marked differently in those two figures. Because those two edges fall on the same line, the Y-plane is 3D, there is no significant change so far the top-to-right brittle shear is concerned.

**Q.5. With reference to Fig. 6A, interchange  $v_3$  and  $v_4$  rows of  $A_1(G)$ . Does the isomorphous graph thus produced have any geological significance?**

There is a second way of representing graphs using matrices: in terms of the "adjacency matrix". Here connection between vertices is presented as follows. The graph in Fig. 6B is presented as:



	$v_1$	$v_2$	$v_3$	$v_4$	$v_5$	$v_6$
$v_1$	0	1	0	0	0	0
$v_2$	1	0	1	0	1	0
$v_3$	0	1	0	0	0	0
$v_4$	0	0	0	0	1	0
$v_5$	0	1	0	1	0	1
$v_6$	0	0	0	0	1	0

The adjacency matrix ( $I$ ) of two disconnected graphs  $I_1$  and  $I_2$  is given by:

$$I = \begin{pmatrix} X(I_1) & 0 \\ 0 & X(I_2) \end{pmatrix}$$

Here  $X(I_i)$ : adjacency matrix for  $I_i$ ; 0: null matrix.

**Q.6. With reference to Fig. 7A, state  $I(G_1)$ ,  $I(G_2)$ , and  $I$ .**

A connected graph that does not contain any cycles is called a *tree*. Edges of the tree are called the *branches* of the tree. Branching out fracture patterns would act as example of a tree. A *forest* is defined by a collection of trees. Several branching out of fractures that are mutually not connected constitutes a forest. The *eccentricity of a vertex* [ $e(v)$ ] is the maximum distance between that vertex and another vertex belonging to the same graph. For example, in Fig. 6B,  $e(v_1) = \text{distances } e_2 + e_3 + e_5$ . The curve length  $e_5$  is considered, and that is not the same as the linear distance between the vertices  $v_5$  and  $v_6$ . The vertex in a graph having minimum eccentricity is called the *center of the graph*. However, this may not be possible to define for all graphs easily. For example, the hexagonal fracture network with length of all fracture segments the same (Fig. 2A), there is no unique vertex that can be called the center of the graph.

**Q.7. For the splay fault case of Fig. 8, find out which vertex can be called the center of the graph.**

A *spanning tree*  $T$  is a sub-group of a graph  $G$ . Such a sub-group consists of all the vertices of  $G$ . We can create spanning trees by selectively deleting a few edges. *But by doing that do we really get geologically meaningful and unique edges?* Let us check this. Fig. 9A is a graph showing a brittle shear zone with top-to-right shear. Deleting its edge  $e_3$  in

FIG. 8 Splay fault network.

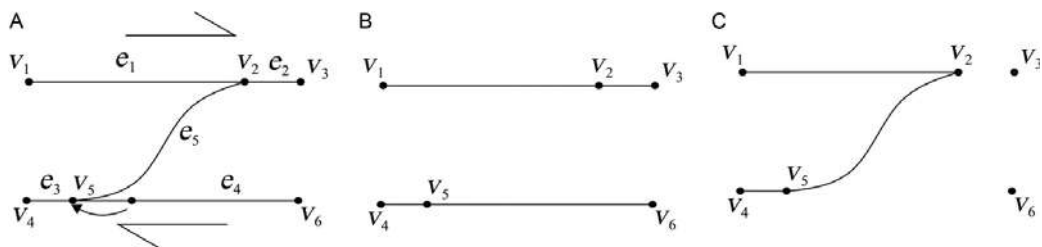
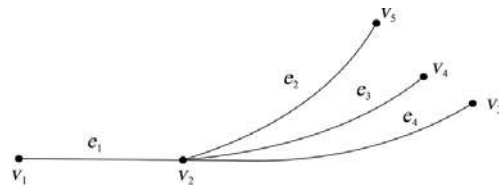


FIG. 9 (A-C) Brittle shear planes in different considerations.

Fig. 9B, we still have all the vertices and only the  $Y$ -planes got separated out. The spanning tree  $T$  in Fig. 9B therefore is geologically meaningful. The edge that is not a part of  $T$  but was a part of  $G$  is called the *tie* or the *chord*. Therefore in the previously mentioned case,  $e_3$  representing the  $P$ -plane is the tie. Fig. 9C is another spanning sub-group of  $G$ , but here uniquely  $P$ - or  $Y$ -planes were not separated out.

One can think of *weight* of edges in a graph, if each edge is assigned some numbers. For example, length of each edge can be assigned as numbers against them.

**Note:** From book to book, the presentation of graph theory varies a little. For example, vertices can be represented by numbers such as 1, 2, etc. An edge that connects the vertices 1 and 2 can be represented by 12 or 21. Students can try to explore the graph theory on branching shear zones as discussed in Meyer et al. (2017) and Passchier and Platt (2017). Few recent papers that students should look at regarding patterns of planes in structural geology are Anders et al. (2014), Peacock et al. (2016, 2018), and Healy et al. (2017).

## SOLUTIONS

**Answer 1A.** Incidence matrix for Fig. 2D:

	$ag$	$gb$	$cf$	$fd$	$fe_1$	$ge_2$
$a$	1	0	0	0	0	0
$b$	0	1	0	0	0	0
$c$	0	0	1	0	0	0
$d$	0	0	0	1	0	0
$e_1$	0	0	0	0	1	0
$e_2$	0	0	0	0	0	1
$f$	0	0	1	1	0	0
$g$	1	1	0	0	0	1

**Answer 1B.** A tiny fracture (Fig. 8), effectively a point, depending on the scale of observation nucleated in a fracture network. This tiny fracture ( $V$ ) can be represented as a single vertex at which no edges are joined. Therefore the row of the binary matrix for this vertex possesses all elements as "0".

**Answer 1C.** Fig. 8. It represents splay faulting. Its incidence matrix is:

	$e_1$	$e_2$	$e_3$	$e_4$
$v_1$	1	0	0	0
$v_2$	1	1	1	1
$v_3$	0	0	0	1
$v_4$	0	0	1	0
$v_5$	0	1	0	0

Note here the second column is represented by only "1". Vertex  $v_2$  is the only vertex connected with all the edges.

**Answer 2.**  $A(G_2)$  is given by:

	$e_1$	$e_2$	$e_3$
$v_1$	1	0	0
$v_2$	1	1	1
$v_3$	0	1	0
$v_4$	0	0	1

$A(G_3)$  is given by:

$$\begin{array}{c} e_4 \\ v_5 \ 1 \\ v_6 \ 1 \end{array}$$

Therefore  $A(G)$  is given by:

$$\begin{array}{c} e_1 \ e_2 \ e_3 \ e_4 \\ v_1 \ 1 \ 0 \ 0 \ \mathbf{0} \\ v_2 \ 1 \ 1 \ 1 \ \mathbf{0} \\ v_3 \ 0 \ 1 \ 0 \ \mathbf{0} \\ v_4 \ 0 \ 0 \ 1 \ \mathbf{0} \\ v_5 \ \mathbf{0} \ \mathbf{0} \ \mathbf{0} \ 1 \\ v_6 \ \mathbf{0} \ \mathbf{0} \ \mathbf{0} \ 1 \end{array}$$

The null matrices are represented by "0".

**Answer 3.** In this case, the number of edges increases to 3.  $A(G)$  is given by:

$$\begin{array}{c} e_1 \ e_2 \ e_3 \\ v_1 \ 1 \ 0 \ 0 \\ v_2 \ 0 \ 0 \ 1 \\ v_3 \ 1 \ 1 \ 1 \\ v_4 \ 0 \ 1 \ 0 \end{array}$$

**Answer 4.** In this case, the number of edges and vertices reduce effectively, and therefore Fig. 7C was modified for vertices and edge naming. Here  $A(G)$  becomes

$$\begin{array}{c} e_1 \ e_2 \ e_3 \\ v_1 \ 1 \ 0 \ 0 \\ v_2 \ 0 \ 0 \ 1 \\ v_3 \ 1 \ \mathbf{0} \ 1 \\ v_4 \ 0 \ \mathbf{0} \ 0 \end{array}$$

The changes that took place in  $A(G)$  from Answer 2 to Answer 3 are shown in the previous matrix in bold. In the present case,  $e_2$ ,  $V_4$  and  $V_3$  lost their independent significance.

**Answer 5.**  $A_1(G) =$

$$\begin{array}{c} e_1 \ e_2 \ e_3 \ e_4 \ e_5 \\ v_1 \ 1 \ 0 \ 0 \ 0 \ 0 \\ v_2 \ 1 \ 1 \ 0 \ 0 \ 1 \\ v_3 \ 0 \ 1 \ 0 \ 0 \ 0 \\ v_4 \ 0 \ 0 \ 1 \ 0 \ 1 \\ v_5 \ 0 \ 0 \ 1 \ 1 \ 0 \\ v_6 \ 0 \ 0 \ 0 \ 1 \ 0 \end{array}$$

Exchanging elements of  $v_3$  and  $v_4$  rows:

	$e_1$	$e_2$	$e_3$	$e_4$	$e_5$
$v_1$	1	0	0	0	0
$v_2$	1	1	0	0	1
$v_3$	0	<b>0</b>	<b>1</b>	0	<b>1</b>
$v_4$	0	<b>1</b>	<b>0</b>	0	<b>0</b>
$v_5$	0	0	1	1	0
$v_6$	0	0	0	1	0

Changes in elements are shown in bold. Drawing the graph the student will find that it has no geological significance.

**Answer 6.**

$I(G_1)=$

	$v_1$	$v_2$
$v_1$	0	1
$v_2$	1	0

$I(G_2)=$

	$v_3$	$v_4$
$v_3$	0	1
$v_4$	1	0

Therefore  $I(G)=$

	$v_1$	$v_2$	$v_3$	$v_4$
$v_1$	0	1	0	0
$v_2$	1	0	0	0
$v_3$	0	0	0	1
$v_4$	0	0	1	0

**Answer 7.** Here  $V_2$  is the center of the graph. Note here the length of the curved edge  $e_2$  equals the eccentricity of  $V_2$  [ $=e(v_2)$ ]. Note  $e(v_2) < e(v_i)$  for  $i \neq 2$ .

Recent review by Peacock and Sanderson (2018) shows several instances where the graph theory can be utilized to represent networks of planes in structural geology.

## Acknowledgments

A research sabbatical for the year 2017 and a CPDA grant provided by IIT Bombay are thanked. Narayan Bose (IIT Bombay) prepared diagrams. Amy Shapiro and Tasha Frank (Elsevier), and Ake Fagereng (Cardiff University) and Andrea Billi (Sapienza University di Roma) are thanked for editorial handling and coordination. Vide the recent paper Sanderson and Nixon (2018) to see how topology and connectivity are explained in the light of flow through fractured media. Vide Mukherjee (in press) to see how graph theory can be used along with Boolean algebra to represent flow network.

## APPENDIX

**Terms Related to Graph Theory Explained in this Article in the Context of Brittle Planes:**

Adjacency matrix, adjacent edges, branch, center of the graph, chain, chord, circuits, close walk, complement of a graph, complete graph, component of a graph, connected graph, degree of the vertex, disconnected graph, distance between vertices, edge, edge disjoint, edge set, edges in a series, end vertices, even vertex, forest, fundamental numbers of a graph, graph, graph theory, incidence matrix, intersection between two graphs, irregular graph, isolated vertex, isomorphic graphs, length of walk, loop, node, node set, null graph, odd vertex, open walk, parallel edges, path, pendant edge, pendant vertex, permutation of columns, permutation of rows, rank, regular graph, self loop, simple graph, simple path, spanning sub-graph, spanning tree, sub-graph, subsets, supergraph, supersets, tie, tree, union between two graphs, vertex disjoint, vertex set, walk, weight.

**References**

- Anders, M.H., Laubach, S.E., Scholz, C.H., 2014. Microfractures: A review. *J. Struct. Geol.* 69, 377–394.
- Bemis, S.P., Micklethwaite, S., Turner, D., James, M.R., Akciz, S., Thiele, S.T., Bangash, H.A., 2014. Ground-based and UAV-Based photogrammetry: a multi-scale, high-resolution mapping tool for structural geology and paleoseismology. *J. Struct. Geol.* 69, 163–178.
- Bollobas, B., 1998. *Modern Graph Theory*. Graduate Texts in Mathematics. Springer. ISBN: 978-0-387-98488-9. pp. 2.
- Corradetti, A., Tavani, S., Parente, M., Iannace, A., Vinci, F., Pirmez, C., Torrieri, S., Giorgioni, M., Pignalosa, A., Mazzoli, S., 2018. Distribution and arrest of vertical through-going joints in a seismic-scale carbonate platform exposure (Sorrento peninsula, Italy): Insights from integrating field survey and digital outcrop model. *J. Struct. Geol.* 108, 121–136.
- Goehring, L., Nakahara, A., Dutta, T., Kitsunezaki, S., Tarafdar, S., 2014. Desiccation Cracks and their Patterns: Formation and Modeling in Science and Nature. Wiley-Vch. ISBN: 978-3-527-41213-6.
- Healy, D., Rizzo, R.E., Cornwell, D.G., Farrell, N.J.C., Watkins, H., Timms, N.E., Gomez-Rivas, E., Smith, M., 2017. FracPaQ: A MATLAB™ toolbox for the quantification of fracture patterns. *J. Struct. Geol.* 95, 1–16.
- Hooker, J.N., Laubach, S.E., Marrett, R., 2018. Microfracture spacing distributions and the evolution of fracture patterns in sandstones. *J. Struct. Geol.* 108, 66–79.
- Howarth, R.J., 2017. *Dictionary of Mathematical Geosciences: With Historical Notes*. Springer, Cham. pp. 245. ISBN: 978-3-319-57314-4.
- Laubach, S.E., Lamarche, J., Gauthier, B.D.M., Dunne, W.M., Sanderson, D.J., 2018. Spatial arrangement of faults and opening-mode fractures. *J. Struct. Geol.* 108, 2–15.
- Li JZ. 2017. *Fracture Spatial Arrangement in Tight Gas Sandstone and Shale Reservoir Rocks*. MS Thesis. The University of Texas at Austin. pp. 1–173.
- Marrett, R., Gale, J.F.W., Gomez, L.A., Laubach, S.E., 2018. Correlation analysis of fracture arrangement in space. *J. Struct. Geol.* 108, 16–33.
- Meyer, S.E., Kaus, B.J.P., Passchier, C., 2017. Development of branching brittle and ductile shear zones: a numerical study. *G Cubed*. 2054–2075. <https://doi.org/10.1002/2016GC006793>.
- Morley, C.K., Nixon, C.W., 2016. Topological characteristics of simple and complex normal fault networks. *J. Struct. Geol.* 84, 68–84.
- Mukherjee, S., 2013a. *Deformation Microstructures in Rocks*. Springer Geochemistry/Mineralogy, Berlin, pp. 1–111. ISBN: 978-3-642-25608-0.
- Mukherjee, S., 2013b. Higher Himalaya in the Bhagirathi section (NW Himalaya, India): its structures, backthrusts and extrusion mechanism by both channel flow and critical taper mechanisms. *Int. J. Earth Sci.* 102, 1851–1870.
- Mukherjee, S., 2014a. *Atlas of Shear Zone Structures in Meso-Scale*. Springer Geology, Cham, pp. 1–124. ISBN: 978-3-319-0088-6.
- Mukherjee, S., 2014b. Review of flanking structures in meso- and micro-scales. *Geol. Mag.* 151, 957–974.
- Mukherjee, S., 2015. *Atlas of Structural Geology*. Elsevier, Amsterdam. ISBN: 978-0-12-420152-1.
- Mukherjee, S., in press. Boolean logic in fluid flow. In: Billi, A., Fagereng, A. (Eds.), *Problems and Solutions in Structural Geology and Tectonics*. In: Mukherjee S. (Ed.), *Developments in Structural Geology and Tectonics Book Series*. Elsevier. ISSN: 2542-9000. ISBN: 9780128140482.
- Pal BK, Das K, 2017. *Engineering Mathematics*. Vol. 2. 11th ed. U.N. Dhur & Sons Pvt. Ltd. Kolkata. pp. 3-1 to 4-94. ISBN: 978-93-80673-16-5.
- Passchier, C.W., Platt, J.P., 2017. Shear zone junctions: of zippers and freeways. *J. Struct. Geol.* 95, 188–202.
- Peacock, D.C.P., Sanderson, D.J., 2018. Structural analyses and fracture network characterisation: seven pillars of wisdom. *Earth Sci. Rev.* 184, 13–28.
- Peacock, D.C.P., Nixon, C.W., Rotevatn, A., Sanderson, D.J., Zuluaga, L.F., 2016. Glossary of fault and other fracture networks. *J. Struct. Geol.* 92, 12–29.
- Peacock, D.C.P., Sanderson, D.J., Rotevatn, A., 2018. Relationship between fractures. *J. Struct. Geol.* 106, 41–53.
- Petford, N., Koenders, M.A.C., 1998. Self-organisation and fracture connectivity in rapidly heated continental crust. *J. Struct. Geol.* 20, 1425–1434.
- Procter, A., Sanderson, D.J., 2018. Spatial and layer-controlled variability in fracture networks. *J. Struct. Geol.* 108, 52–65.
- Sanderson, D.J., Nixon, C.W., 2018. Topology, connectivity and percolation in fracture networks. *J. Struct. Geol.* 115, 167–177.
- Sanderson D.J., Peacock D.C.P., Nixon C.W. and Rotevatn A., Graph theory and the analysis of fracture networks, *J. Struct. Geol.* in press, <https://doi.org/10.1016/j.jsg.2018.04.011>.
- Watkins, H., Bond, C.E., Healy, D., Butler, R.W.H., 2015. Appraisal of fracture sampling methods and a new workflow to characterise heterogeneous fracture networks at outcrop. *J. Struct. Geol.* 72, 67–82.
- Watkins, H., Healy, D., Bond, C.E., Butler, W.H., 2018. Implications of heterogeneous fracture distribution on reservoir quality: an analogue from the Torridon Group sandstone, Moine Thrust Belt, NW Scotland. *J. Struct. Geol.* 108, 180–197.